

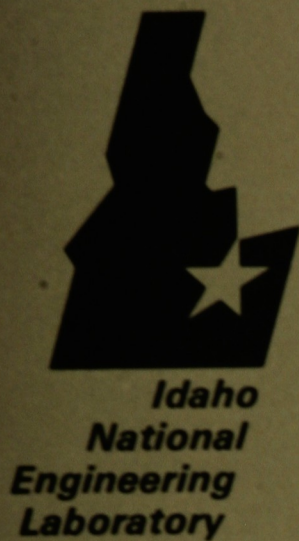
EGG-TMI-7987

EGG-TMI-7987  
April 1988

## INFORMAL REPORT

TMI-2 B-LOOP STEAM GENERATOR  
LOOSE DEBRIS EXAMINATIONSS

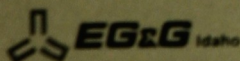
C. V. McIsaac  
G. S. Roybal  
A. W. Marley



Managed  
by the U.S.  
Department  
of Energy


LOAN COPY

THIS REPORT MAY BE RECALLED  
AFTER TWO WEEKS PLEASE  
RETURN TO THE LIBRARY



Work performed under  
DOE Contract  
No. DE-AC07-78ID01570

#### DISCLAIMER

This book was prepared as an account of work sponsored by an agency of the United States Government. Neither the United States Government nor any agency thereof, nor any of their employees, makes any warranty, express or implied, or assumes any legal liability or responsibility for the accuracy, completeness, or usefulness of any information, apparatus, product or process disclosed, or represents that its use would not infringe privately owned rights. References herein to any specific commercial product, process, or service by trade name, trademark, manufacturer, or otherwise, does not necessarily constitute or imply its endorsement, recommendation, or favoring by the United States Government or any agency thereof. The views and opinions of authors expressed herein do not necessarily state or reflect those of the United States Government or any agency thereof.

TMI-2 B-LOOP STEAM GENERATOR  
LOOSE DEBRIS EXAMINATIONS

C. V. McIsaac  
G. S. Roybal  
A. W. Marley

Published April 1988

EG&G Idaho, Inc.  
Idaho Falls, Idaho 83415

Prepared for the  
U.S. Department of Energy  
Idaho Operations Office  
Under DOE Contract No. DE-AC07-76ID01570



## ABSTRACT

This report presents the results of the examination and analysis performed on a sample of loose, gravel-like particulate debris collected during March 1987 from the top of the B-loop steam generator upper tube sheet of the TMI-2 reactor. The examination and analysis is part of the characterization of the TMI-2 reactor coolant system being performed by EG&G Idaho and GPU Nuclear Corporation.

Results of the analysis indicate that the recovered debris is similar to the samples of debris collected from the upper core debris bed. The debris, which was probably transported from the reactor vessel to the B-loop steam generator when the 2-B reactor coolant pump was turned on 174 minutes into the accident, was examined to define its physical characteristics, composition, and associated radionuclide concentrations.



## CONTENTS

ABSTRACT .....	11
1. INTRODUCTION .....	1
2. SAMPLE ACQUISITION AND ANALYTICAL METHODS .....	6
2.1 Sample Acquisition .....	6
2.2 Analytical Methods .....	6
2.2.1 Physical Examinations .....	9
2.2.2 Gamma Ray Spectroscopy Measurements .....	10
2.2.3 Fissile Material Assays .....	10
2.2.4 Chemical and Radiochemical Analyses .....	11
3. EXAMINATION RESULTS/DISCUSSION .....	13
3.1 Physical Examinations .....	13
3.2 Radiochemical Analyses .....	16
3.3 Elemental Analyses .....	24
4. OBSERVATIONS AND CONCLUSIONS .....	30
5. REFERENCES .....	32

## FIGURES

1. Reactor coolant system piping and components .....	5
2. Apparatus used to collect the loose debris sample .....	7
3. Vacuum nozzle arrangement .....	8
4. Particle-size distribution .....	14
5. Radionuclide and U-235 concentrations as a function of particle size .....	18
6. Element concentrations as a function of particle size .....	27

## TABLES

1.	Results of particle-size analysis of the B-loop steam-generator debris sample .....	15
2.	Masses of the samples analyzed .....	15
3.	Concentrations of radionuclides and U-235 in debris collected from the B-loop steam-generator upper tube sheet .....	17
4.	Radionuclide concentrations normalized to uranium concentrations ( $\mu\text{Ci/g U}$ ) .....	21
5.	Retentions of fission products based on their theoretical core average concentrations in the fuel .....	23
6.	Concentrations of elements in debris collected from the B-loop steam generator upper tube sheet (Wt%) .....	25

## TMI-2 B-LOOP STEAM GENERATOR LOOSE DEBRIS EXAMINATIONS

### 1. INTRODUCTION

The Unit-2 pressurized water reactor at Three Mile Island (TMI-2) experienced a loss-of-coolant accident on March 28, 1979, that resulted in severe damage to the core. Since the accident, considerable effort has been expended to improve our understanding of the physical mechanisms that controlled the core damage progression and to assess the magnitude of the release of fission products and fuel from the active core region to the reactor coolant system (RCS) and other auxiliary systems. This report presents the results of the examinations and analyses performed on a sample of loose particulate debris collected during March 1987 from the top of the B-loop steam generator upper tube sheet. The objective of these examinations was to characterize the composition and fission product concentrations of debris transported out of the reactor vessel to the RCS, probably during the operation of the "B" reactor coolant pump.

The first visual inspections of the core were performed during 1982 using a closed-circuit television (CCTV) system.<sup>1</sup> The inspections revealed the presence of a large void in the upper region of the core. The void extended axially about 160 cm into the active fuel region and radially, in some locations, to the core former wall, occupying approximately 25% of the original core region. Relatively intact fuel rods were observed in the peripheral regions of the core and a bed of granular rubble was seen to extend over most of the diameter of the core. After the CCTV inspection on August 12, 1982, the debris bed was probed by lowering a stainless steel rod through two control rod guide tube openings. The probes indicate that the debris bed was as deep as 94 cm and that it rested on a hard layer of solidified core material.

Following the success of the exploratory probings, the first samples of debris bed material were collected during September and October 1983. At this time, a total of six samples were retrieved from the debris bed at grid locations H8 and E9, which were, respectively, near the center and



mid-radius of the core. At each location, samples were collected from the surface of the bed and at depths of 8 and 56 cm below the surface of the debris bed. Five additional samples were extracted from the debris bed at these same two locations during March 1984. Samples were collected at depths of 74 and 94 cm at location E9 and at depths of 36, 70, and 77 cm at location H8.

In order to complete the end-state characterization of the reactor core, a core boring machine similar in design to the boring machines employed to extract geological core samples was built and subsequently used during July and August 1986 to drill through the entire height of the core at ten different locations.<sup>2</sup> At nine of these locations, core samples measuring 6.4 cm in diameter by about 1.8 m in length were extracted from the reactor core. Immediately following the removal of each of the nine core samples, the core bore hole was visually inspected using a CCTV system. The inspections revealed that the damage to the core was much more extensive than originally estimated. A region of previously molten material having a volume estimated to be about 10% of the original core volume was confirmed to be in the lower, central region of the core. The solid structure was about 1.2-m thick at the center of the core, and it tapered to a thickness of between about 30 and 60 cm near the core periphery. Sections of standing intact fuel rods were present between the bottom surface of the solid ceramic structure and the fuel rod lower endfittings. Inspections of the lower plenum region revealed that from 10 to 20 metric tons of previously molten material were present in the reactor vessel lower plenum below the flow distributor plate.

The examinations of the reactor core described above provided a basis for postulating a credible accident scenario that includes core damage progression during the accident.<sup>3</sup> Two fundamental features of the accident scenario that will be useful in interpreting the results of the analyses of the debris collected from the B-loop steam generator are summarized below:

1. The Zircaloy-4 cladding in the upper half of the core experienced rapid heatup and oxidation between 150 and 174 min into the accident. During this time frame, temperatures near the center of the core were sufficient to cause Zircaloy-4 cladding to melt. The molten cladding dissolved some of the  $\text{UO}_2$ , and this molten U-Zr-O ternary mixture flowed toward the lower region of the core where it solidified when it came into contact with reactor coolant in the bottom of the vessel. The end-state configuration of the ceramic monolith in the core indicates that cooling in the lower 0.5 m of the core was maintained. By 174 min, the region of molten materials and severely damaged fuel assemblies included about one-third of the total quantity of materials in the core.
2. When the B-2 reactor coolant pump was turned on momentarily at 174 min, as much as  $28 \text{ m}^3$  of water was injected into the core in less than 15 s. The resulting thermal shock and the mechanical forces born from rapid steam production probably shattered the oxidized fuel rod remnants above the molten region, forming a bed of debris across most of the diameter of the core. At 200 min, the high-pressure injection system (HPIS) was turned on. Although the exact amount of water injected by the HPIS is not known, best estimates indicate that sufficient quantities of water were injected from these two sources to cover the core sometime after 200 min.

The video inspections of the core bore holes indicate that remnants of fuel assembly structures originally located at the upper ends of the fuel assemblies were embedded in the upper crust of the previously molten ceramic structure, which was buried under as much as 94 cm of granular debris. This is strong evidence that the debris bed was vigorously mixed before the upper crust formed sometime after 200 min into the accident.

Figure 1 shows the TMI-2 reactor coolant system piping and components. Each of the two reactor coolant loops consists of a once-through steam generator, two reactor coolant pumps, and associated hot- and cold-leg piping. The figure shows the flowpath of reactor coolant through the system when operated under normal operating conditions. Reactor coolant discharged from a reactor coolant pump is routed to the reactor vessel through a cold leg. Upon entering the reactor vessel, the coolant is directed via a downcomer to the bottom of the reactor vessel. From the lower reactor vessel head it flows up through a flow distributor plate and thence through the reactor core. After exiting the top of the core, the coolant leaves the reactor vessel and is routed to the tops of the steam generators via two candy-cane-shaped hot legs. Each hot-leg rises more than 14 m between the reactor vessel outlet and the steam generator inlet. Given the fact that the B-loop hot-leg is the only pathway by which core particulate debris could have reached the upper tube sheet of the B-loop steam generator, it is almost certain that the material was deposited on the tube sheet during the brief time the 2-B reactor coolant pump was turned on 174 min into the accident.

Forced circulation cooling of the reactor core was resumed about 16 h after the initiation of the accident through the A-loop using reactor coolant pump 1-A. Natural circulation cooling of the core commenced about 31 days after accident initiation with coolant flowing through both the A- and B-loops. The B-loop steam generator was later isolated. Beginning 2 years and 106 days after the accident, an equivalent of 4 reactor coolant system volumes of reactor coolant was processed through the SES/EPICOR-II system. The steam generator tubesheets were uncovered during July 1982 when the reactor coolant system water level was lowered for initial reactor disassembly. During the 3 years and 4 months that the debris on the upper tube sheet of the B-loop steam generator was submerged in reactor coolant, the pH of the reactor coolant was maintained between 7.5 and 7.7.<sup>4</sup>



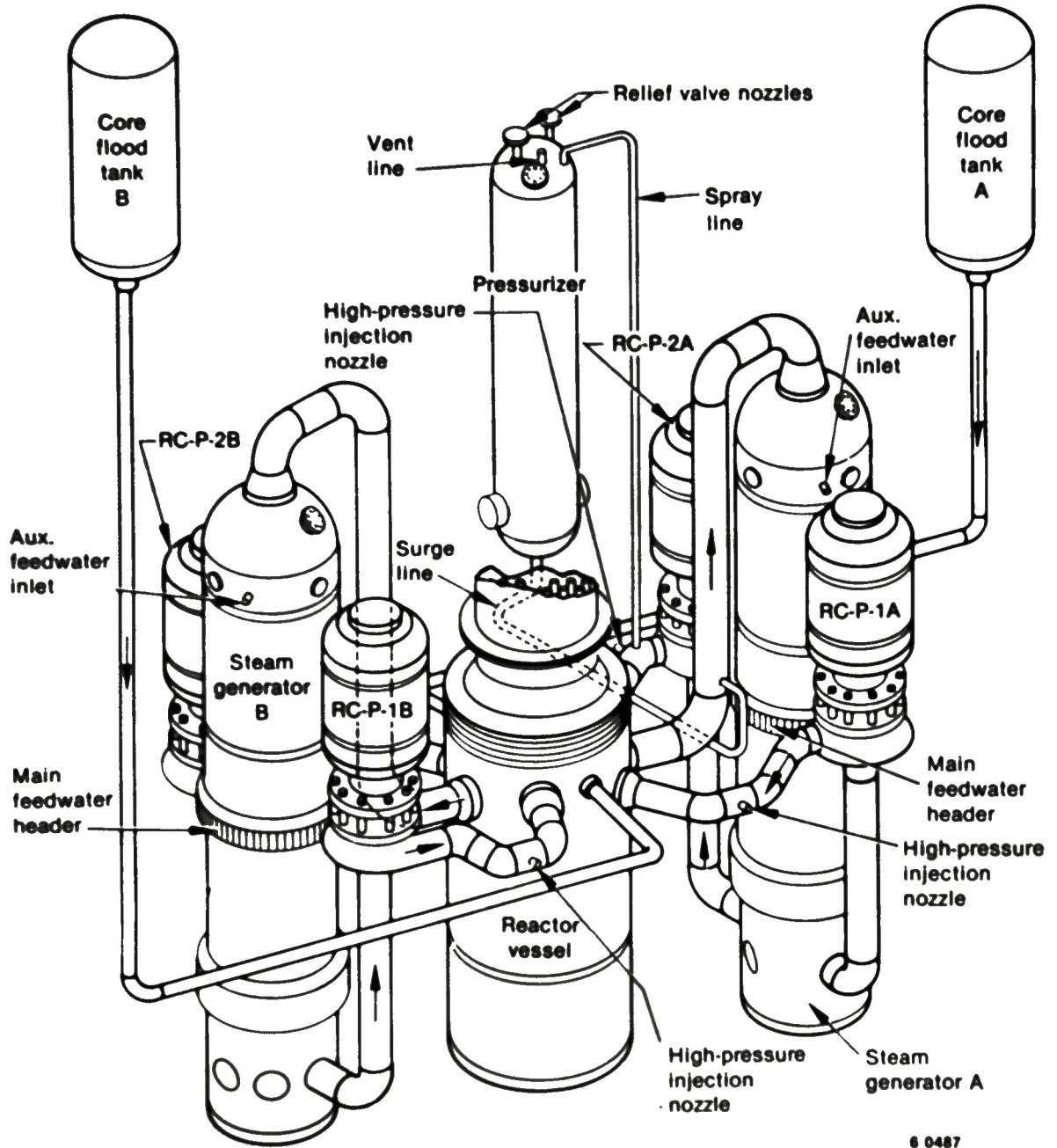


Figure 1. Reactor coolant system piping and components.

## 2. SAMPLE ACQUISITION AND ANALYTICAL METHODS

This section describes the procedure and the apparatus used to retrieve loose particulate matter from the upper tube sheet of the "B" steam generator, and it also describes the analytical methods used to analyze the sample after it arrived at the Idaho National Engineering Laboratory (INEL).

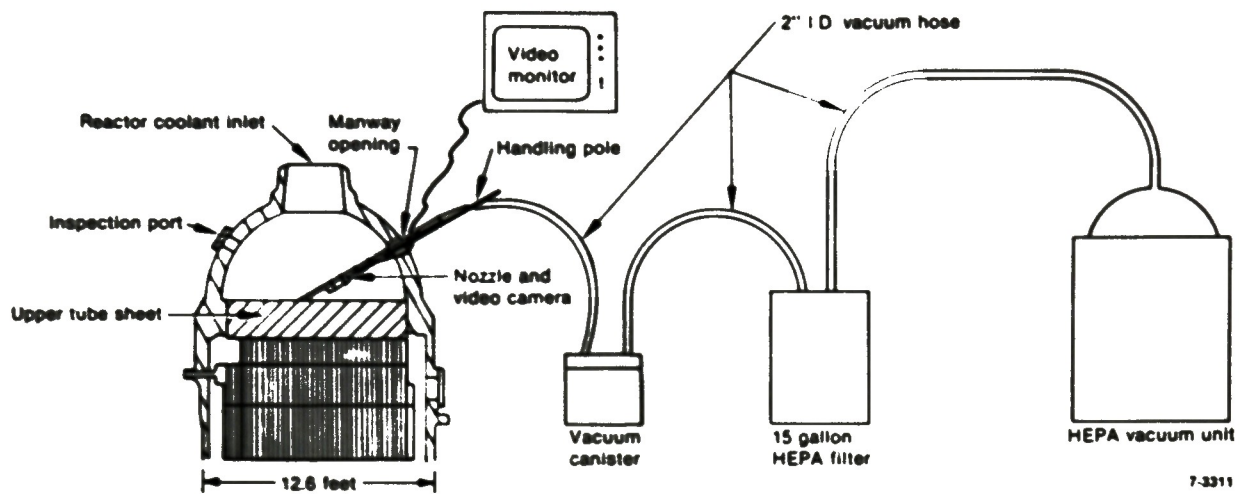
### 2.1 Sample Acquisition

In March 1987 about 81 g of loose particulate debris were retrieved from the top surface of the B-loop steam generator upper tube sheet, using a vacuum apparatus shown schematically in Figure 2. The vacuum apparatus was equipped with a suction nozzle that consisted of a 2.4-m-long Al pipe having a 1.58-cm inside diameter. Figure 3 is a schematic of the vacuum nozzle. As shown in Figure 2, the nozzle with an attached video camera was inserted into the upper plenum of the steam generator through the manway opening.

The sample of loose particulate debris was sucked from the top of the tube sheet through the nozzle pipe and vacuum hose into a polypropylene sock-type filter where it was trapped. The filter was supported by a perforated stainless steel canister that measured 10.2 cm in diameter by 20.3 cm in length. The perforated canister was installed inside an outer filter canister that was shielded with Pb and had special features so that it could be used as an R2-type shipping container.

### 2.2 Analytical Methods

The vacuum canister was shipped to the INEL where the sample was unloaded, separated into sieve fractions, and weighed. When the sample canister was opened, it was determined that the polypropylene filter was torn and that some of the debris had fallen to the bottom of the canister. Inquiries at TMI-2 indicated that the filter may have broken during operation and that some of the smaller particle size material may have been lost. The filter sleeve and approximately one-half of the sample,



7-3311

Figure 2. Apparatus used to collect the loose debris sample.



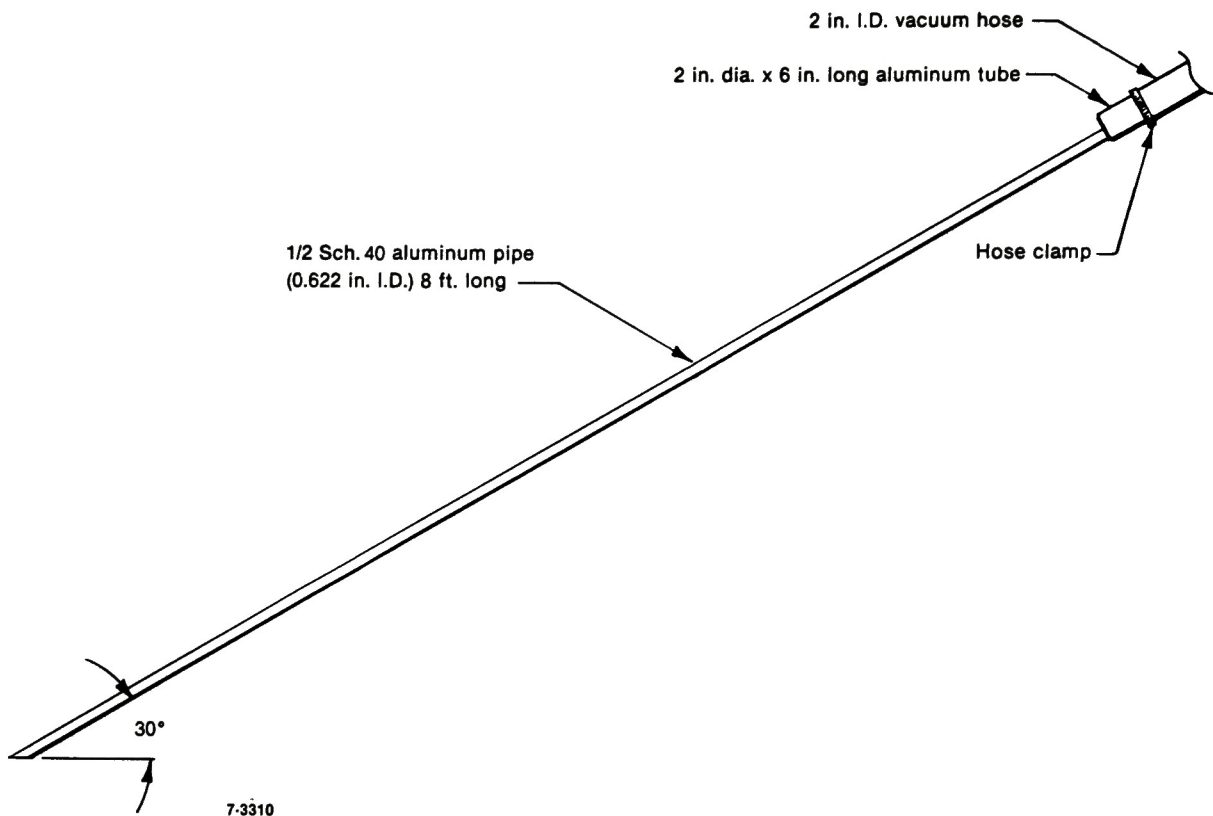


Figure 3. Vacuum nozzle arrangement.

including the largest individual particle, were repackaged into the vacuum canister and transported to Babcock and Wilcox (B&W) in Lynchburg, Virginia, for examination. The analytical methods used at the INEL in analyzing the sample included particle sizing, using sieves, gamma ray spectroscopy, neutron activation analysis, flow-through gas proportional counter analysis of beta emitting species, and elemental analysis, using inductively coupled plasma (ICP) spectroscopy. These analytical techniques were, in most cases, standard laboratory techniques.

In total, twelve individual sample aliquots were analyzed. Eleven of the twelve samples were of particles having specific sizes, and one was the recombined bulk sample. The latter sample was to have been analyzed to determine the average concentrations of the radionuclides and elements in the bulk sample; however, because of analysis problems, the radiochemical analysis results are not included in this report.

#### 2.2.1 Physical Examinations

Visual examinations of the debris sample were performed and photographs were taken during unpackaging and throughout the handling of the sample to determine the sizes, shapes, and types of particles in the sample. Following the initial examinations, the sample was dried at 100° C and was then weighed.

The particle-size distribution of the bulk sample was performed using a column of five progressively smaller sieves. The sieves, manufactured by Dual Manufacturing Company, Chicago, Illinois, were a United States standard sieve series meeting A.S.T.M. E-11 specifications. After transferring the dried bulk sample to the sieve column, the column was shaken for several minutes to segregate it into particle-size fractions according to sieve aperture size. The sieve sizes used were 1000, 710, 300, and 150  $\mu\text{m}$ ; the bulk sample was segregated into the following size fractions: >1000  $\mu\text{m}$ , <1000 to >710  $\mu\text{m}$ , <710 to >300  $\mu\text{m}$ , <300 to >150  $\mu\text{m}$ , and <150  $\mu\text{m}$ . Each size fraction was examined visually, weighed, and then divided in half. One half of each size fraction was transported to B&W.

In the case of the >1000  $\mu\text{m}$  size fraction, 7 individual particles having a total mass of 1.39 g were extracted from the sample for analysis. The masses of these individual particles ranged from 0.076 to 0.258 g. These samples were chosen based on a fuel pellet-like appearance to characterize radionuclide concentrations in fuel transported to the RCS. All of the other size fractions analyzed consisted of multiple particles.

### 2.2.2 Gamma Ray Spectroscopy Measurements

Gamma ray spectroscopy analyses were performed on the 7 individual particles removed from the >1000  $\mu\text{m}$  size fraction and on each of the other four size fractions. These analyses were performed by the Radiation Measurements Laboratory (RML) using an HPGe spectrometer controlled by a VAX 11/750 computer. All spectra were analyzed using GAP,<sup>5</sup> a pulse-height gamma ray analysis program designed for, and used routinely on, the RML VAX 11/750. The calibration of the HPGe gamma-ray spectrometer used to analyze the debris samples was routinely checked using traceable standards obtained from the National Bureau of Standards.

### 2.2.3 Fissile Material Assays

The quantities of fissile material (i.e., U-235) in the five particle size fractions of the debris sample were determined using a delayed neutron counting technique,<sup>6</sup> and samples were analyzed using the delayed neutron counting system at the Advanced Reactivity Measurement Facility (ARMF). The delayed neutron counting system uses the 100-kW reactor at the ARMF, and uses a pneumatic sample transport system that rapidly moves the sample from the reactor to the delayed neutron counter. The system was calibrated using standards containing known quantities of U-235 and -238. The U-235 count rate data for the samples were corrected for background, self-shielding, and delayed neutron counts resulting from the fission of U-238 and Pu-239. For each sample, a U-235 enrichment of 2.64 Wt% was assumed so that the gross count rate could be corrected (2-3%) for the count rate resulting from U-238. The corrected count rate data were



converted to U-235 equivalent masses, using the delayed neutron counting system calibration functions. These U-235 equivalent masses were for the amount of Pu-239 present in each sample. As of March 1979, Pu-239 averaged 7.3% of the total fissile material in the core;<sup>7</sup> therefore, in each case, 92.7% of the U-235 equivalent mass was assumed to be U-235.

#### 2.2.4 Chemical and Radiochemical Analyses

Seven individual particles from the >1000  $\mu\text{m}$  size fraction and one aliquot from each the four smaller size fractions were analyzed for I-129, Sr-90, and core material elements. Prior to analysis, the samples were dissolved, using a pyrosulfate fusion technique initially developed to analyze the core debris grab samples.<sup>8</sup> This dissolution is performed in a closed system to contain the volatile I-129. Also, stable iodine carrier is added to each sample prior to dissolution to minimize the loss of I-129 during the dissolution, and I-131 is added to determine the chemical yield of I-129. A buffered sodium hydroxide solution is used to trap the gaseous I-129 and -131 that evolves from the sample during dissolution. The iodine is then removed from the solution, using standard chemical separation methods and an anion exchange column to extract the iodine from the solution. The ion exchange resin is subsequently activated in the ARMF reactor, producing I-130, which can be measured using gamma spectroscopy. Iodine-130 is an activation product of I-129, and, therefore, the amount of I-129 in the sample is proportional to the quantity of I-130 measured.

The concentration of Sr-90 is determined by placing the nonvolatile portion of the dissolved sample in solution in water, adding a known quantity of Sr carrier, and precipitating the Sr-90 and Sr carrier as Sr-carbonate. The strontium is then separated from its yttrium daughter product (a gamma ray emitter) and the concentration of strontium is determined by the increase in the amount of measurable yttrium in the sample.

The concentrations of stable elements in the nonvolatile portion of each sample are determined using inductively coupled plasma (ICP)

spectroscopy. The concentrations of the following elements were measured: Ag, Al, B, Cd, Cr, Cu, Fe, Gd, In, Mn, Mo, Ni, Nb, Si, Sn, Te, U, and Zr. These elements and O are the major elements in the materials that make up the reactor core.

### 3. EXAMINATION RESULTS/DISCUSSION

This section presents the results of the physical examinations, gamma ray spectroscopy measurements, fissile material assays, and chemical and radiochemical analyses described in Section 2.

#### 3.1 Physical Examinations

The particle-size distribution of the bulk sample (40 g) was determined using the method described in Section 2.2.1. Results of the particle-size distribution analysis are presented in Table 1 and are plotted in Figure 4. The data in Table 1 show that 93.3 Wt% of the debris sample consists of particles larger than 1000  $\mu\text{m}$ . The weight percents of the four remaining size fractions are: (1) >710 to <1000  $\mu\text{m}$ , 1.7 Wt%; (2) >300 to <710  $\mu\text{m}$ , 2.7 Wt%; (3) >150 to <300  $\mu\text{m}$ , 1.0 Wt%, and (4) <150  $\mu\text{m}$ , 1.3 Wt%. This particle-size distribution is similar to the particle-size distributions that were determined for 7 of the 11 samples of particulate matter that were removed from the core debris bed during 1983 and 1984. For seven of the debris bed samples, greater than 80% of their masses were made up of particles larger than 1000  $\mu\text{m}$ .<sup>8</sup> However, these data may not accurately define the particle-size distribution for the sample, as was noted, because the sock-like filter containing the sample had failed and some of the smaller particle size material may have been lost.

The particles larger than 1000  $\mu\text{m}$  generally had sharp angular surfaces and were a medium grey color. The masses of the 7 particles from this size range that were individually analyzed for concentrations of radionuclides and elements ranged from 0.076 to 0.258 g. The masses of these 7 individual particles and the masses of the samples from the four smaller size ranges are presented in Table 2. The data in Table 2 show that, excluding the recombined bulk sample, the total mass of the particle-size fractions that were analyzed is about 1.6 g, and the cumulative mass of the 7 particles larger than 1000  $\mu\text{m}$  is about 85% of this total, being about 1.4 g.

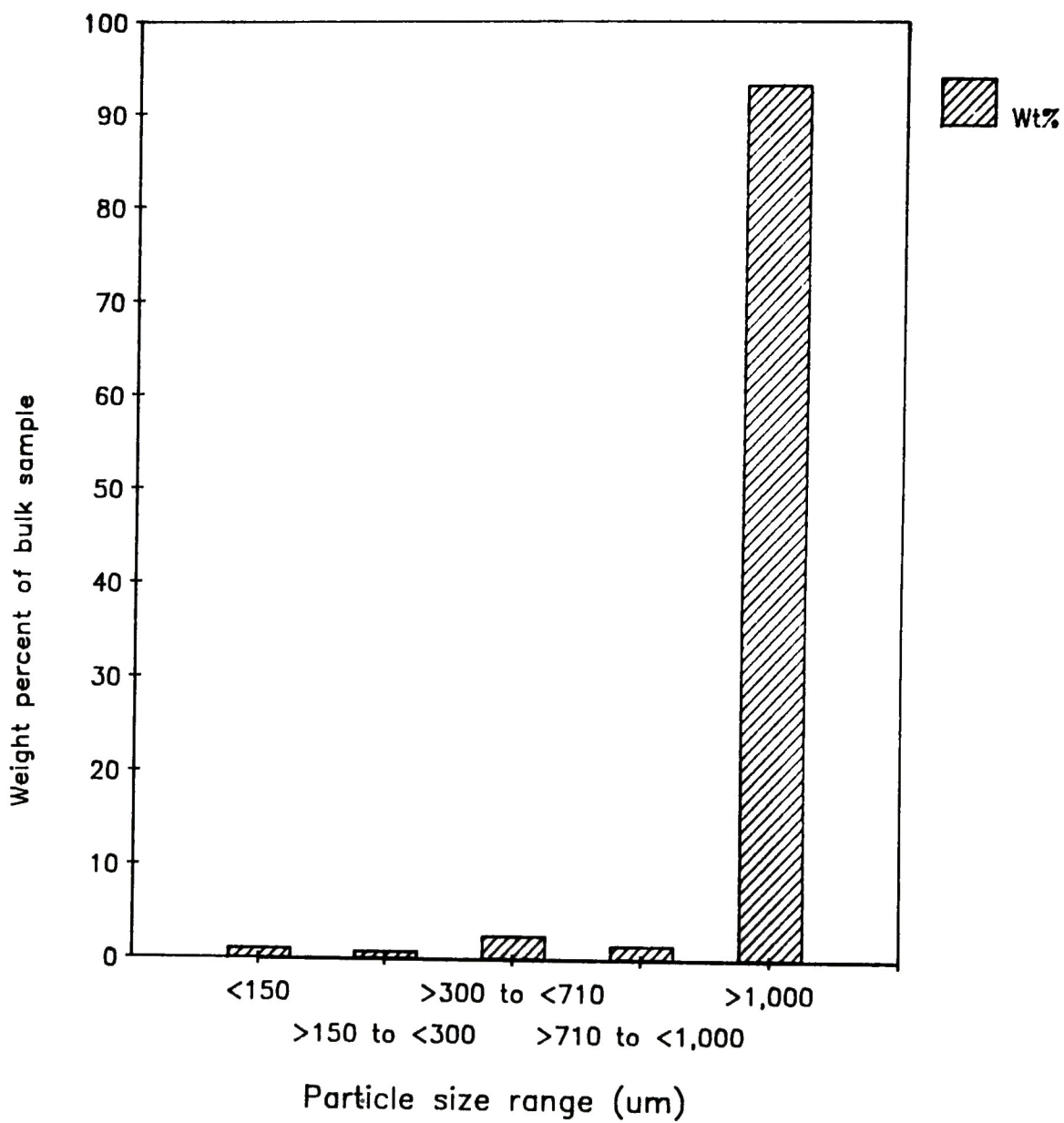


Figure 4. Particle-size distribution.



TABLE 1. RESULTS OF THE PARTICLE-SIZE ANALYSIS OF THE B-LOOP STEAM GENERATOR DEBRIS SAMPLE

Particle Size ( $\mu\text{m}$ )	Original Bulk Sample		Recombined Bulk Sample	
	Mass (g)	(Wt%)	Mass (g)	(Wt%)
>1000	75.600	93.3	38.140	94.6
>710 to >1000	1.350	1.7	0.497	1.2
>300 to >710	2.200	2.7	0.934	2.3
>150 to >300	0.796	1.0	0.215	0.5
>150	1.077	1.3	0.546	1.4
Total mass	81.023		40.322	

TABLE 2. MASSES OF THE SAMPLES THAT WERE ANALYZED

Particle Size ( $\mu\text{m}$ )	Sample Mass (g)
>150	0.037
>150 to >300	0.055
>300 to >710	0.119
>710 to >1000	0.040
>1000	0.076
>1000	0.223
>1000	0.134
>1000	0.226
>1000	0.230
>1000	0.258
>1000	0.240

### 3.2 Radiochemical Analyses

Radiochemical analyses were performed on 7 individual particles segregated from the >1000  $\mu\text{m}$  size fraction, on aliquots from 4 sieve fractions smaller than 1000  $\mu\text{m}$ , and on the recombined bulk sample. The samples from each particle-size fraction were subjected to various analyses to determine the concentrations of gamma-emitting radionuclides, U-235, Sr-90, and I-129. With the exception of neutron activation analysis for I-129, the recombined bulk sample was subjected to the same analyses as the particle-size fractions.

The concentrations of Co-60, Sr-90, Ru-106, Sb-125, I-129, Cs-134, Cs-137, Ce-144, Eu-154, Eu-155, and U-235 measured in the eleven samples analyzed are presented in Table 3. The concentrations are reported as  $\mu\text{Ci/g}$  for the fission and activation products, and as  $\mu\text{g/g}$  for U-235. All activities are decay-corrected to April 1, 1987. The average concentrations measured in the 7 particles larger than 1000  $\mu\text{m}$  are also presented in Table 3. Radionuclide and U-235 concentrations for the four particle size fractions smaller than 1000  $\mu\text{m}$ , and the average radionuclide and U-235 concentrations measured for the 7 particles larger than 1000  $\mu\text{m}$  are plotted as a function of particle-size range in Figure 5.

The plots shown in Figure 5 indicate that the concentrations of Ru-106, Sb-125, I-129, Cs-137, and Eu-155 are highest in particles smaller than 150  $\mu\text{m}$ . For example, the concentration of Cs-137 is about 6 mCi/g in particles smaller than 150  $\mu\text{m}$  and is about one half that value in the larger particles, ranging from about 2.1 mCi/g for particles between 710 and 1000  $\mu\text{m}$  to 3.0 mCi/g for particles larger than 1000  $\mu\text{m}$ . Similarly, the concentration of I-129 is about 81 pCi/g for the smallest particle-size range, whereas its concentrations in the four successively larger particle-size ranges are about 11, 6, 44, and 6 pCi/g, respectively. For spherical particles, the surface-area-to-mass ratio is inversely proportional to particle radius, which implies that if density is reasonably uniform, a given mass of 150- $\mu\text{m}$  particles will have about

TABLE 3. CONCENTRATIONS OF RADIONUCLIDES AND U-235 IN DEBRIS SAMPLE COLLECTED FROM THE "B" STEAM GENERATOR  
UPPER TUBE SHEET<sup>a</sup>

Particle Size (µm)	Sample Mass (g)	[µCi/g]										[mg/g]	
		Cs-60	Sr-90	Ru-106	Sb-125	I-129	Cs-134	Cs-137	Cg-144	Pu-144	Pu-154	Pu-235	U-235
<150	3.700 ± 0.2	1.22 ± 0.1	4.11 ± 0.3	1.61 ± 0.2	7.69 ± 0.2	8.08 ± 0.2	1.19 ± 0.2	6.03 ± 0.3	1.52 ± 0.2	2.69 ± 0.1	3.94 ± 0.1	1.55 ± 0.4	
>150 to <300	5.480 ± 0.2	6.87 ± 0.1	3.76 ± 0.3	4.91 ± 0.1	2.23 ± 0.2	1.05 ± 0.2	5.66 ± 0.1	2.77 ± 0.3	1.78 ± 0.2	2.39 ± 0.1	1.61 ± 0.1	1.17 ± 0.4	
>300 to <710	1.185 ± 0.1	5.13 ± 0.1	3.10 ± 0.3	5.78 ± 0.1	1.98 ± 0.2	6.04 ± 0.3	5.98 ± 0.1	2.91 ± 0.3	1.33 ± 0.2	2.94 ± 0.1	1.70 ± 0.1	1.33 ± 0.4	
>710 to <1,000	4.010 ± 0.2	7.70 ± 0.1	5.99 ± 0.3	6.38 ± 0.1	4.70 ± 0.1	4.35 ± 0.2	3.86 ± 0.1	2.06 ± 0.3	1.80 ± 0.2	3.75 ± 0.1	2.18 ± 0.1	1.69 ± 0.4	
>1,000	7.630 ± 0.2	1.45 ± 0.1	2.09 ± 0.3	2.75 ± 0.0	2.58 ± 0.1	2.48 ± 0.3	2.61 ± 0.1	1.51 ± 0.1	6.67 ± 0.1	8.64 ± 0.0	1.53 ± 0.1	9.33 ± 0.3	
>1,000	2.233 ± 0.1	3.04 ± 0.1	7.75 ± 0.3	1.23 ± 0.2	6.23 ± 0.1	2.50 ± 0.4	8.64 ± 0.1	5.66 ± 0.3	2.19 ± 0.2	2.73 ± 0.1	1.04 ± 0.1	2.33 ± 0.4	
>1,000	1.342 ± 0.1	3.05 ± 0.0	1.09 ± 0.4	1.52 ± 0.2	4.16 ± 0.1	3.84 ± 0.3	3.46 ± 0.1	1.66 ± 0.3	2.38 ± 0.2	4.68 ± 0.1	2.39 ± 0.1	2.27 ± 0.4	
>1,000	2.264 ± 0.1	6.46 ± 0.0	5.05 ± 0.3	1.07 ± 0.2	4.79 ± 0.1	4.54 ± 0.3	2.73 ± 0.1	1.66 ± 0.3	1.77 ± 0.2	2.51 ± 0.1	1.76 ± 0.1	2.21 ± 0.4	
>1,000	2.303 ± 0.1	1.63 ± 0.1	4.49 ± 0.3	5.17 ± 0.0	1.02 ± 0.1	7.51 ± 0.4	1.19 ± 0.1	6.40 ± 0.2	1.28 ± 0.2	4.87 ± 0.0	1.87 ± 0.1	1.50 ± 0.4	
>1,000	2.579 ± 0.1	5.39 ± 0.1	7.19 ± 0.3	1.35 ± 0.2	6.64 ± 0.1	1.60 ± 0.2	1.05 ± 0.2	5.97 ± 0.3	2.47 ± 0.2	3.30 ± 0.1	1.40 ± 0.1	2.38 ± 0.4	
>1,000	2.400 ± 0.1	8.77 ± 0.1	1.60 ± 0.3	1.07 ± 0.2	5.70 ± 0.1	1.53 ± 0.2	7.91 ± 0.1	5.26 ± 0.3	1.59 ± 0.2	2.76 ± 0.1	1.06 ± 0.1	2.34 ± 0.4	

a. Activities are decay corrected to April 1, 1987.

b. Average concentrations of >1,000 µm particles only.

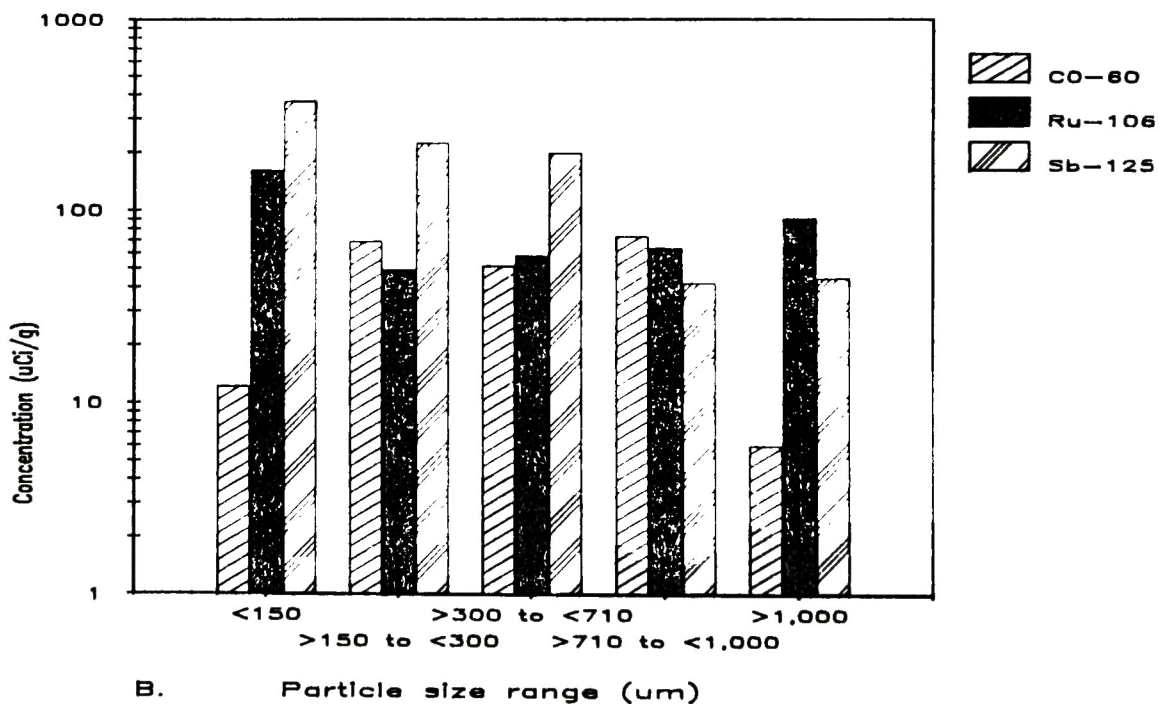
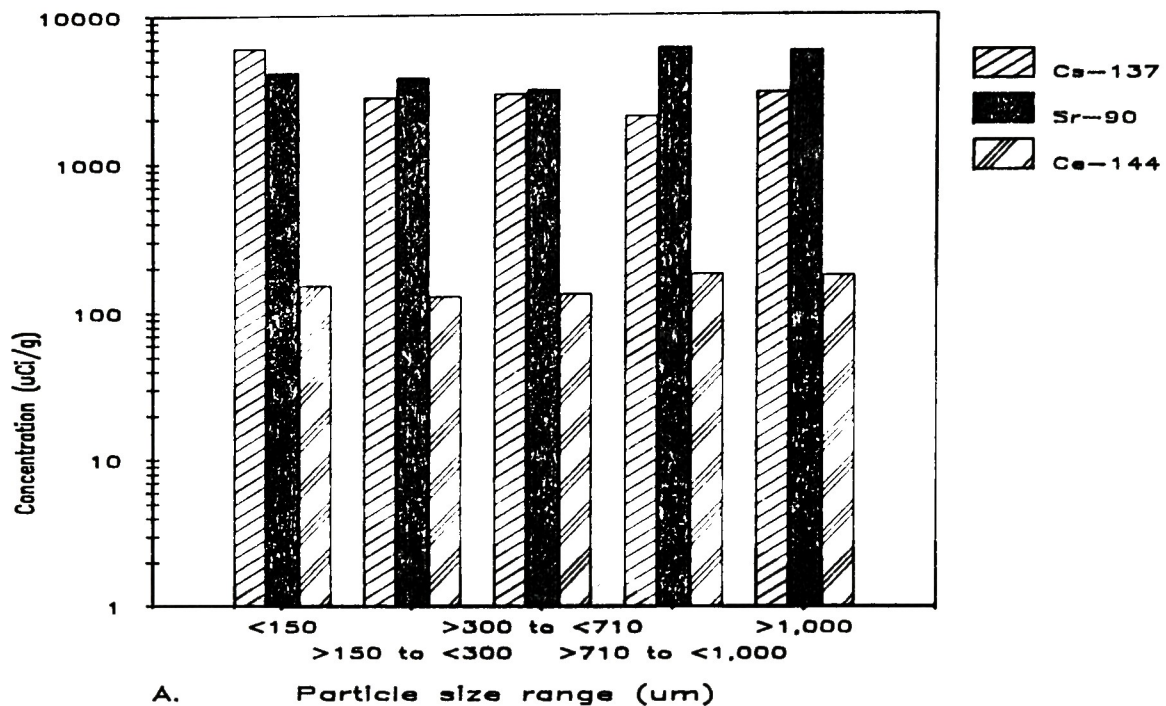


Figure 5. Radionuclide and U-235 concentrations as a function of particle size



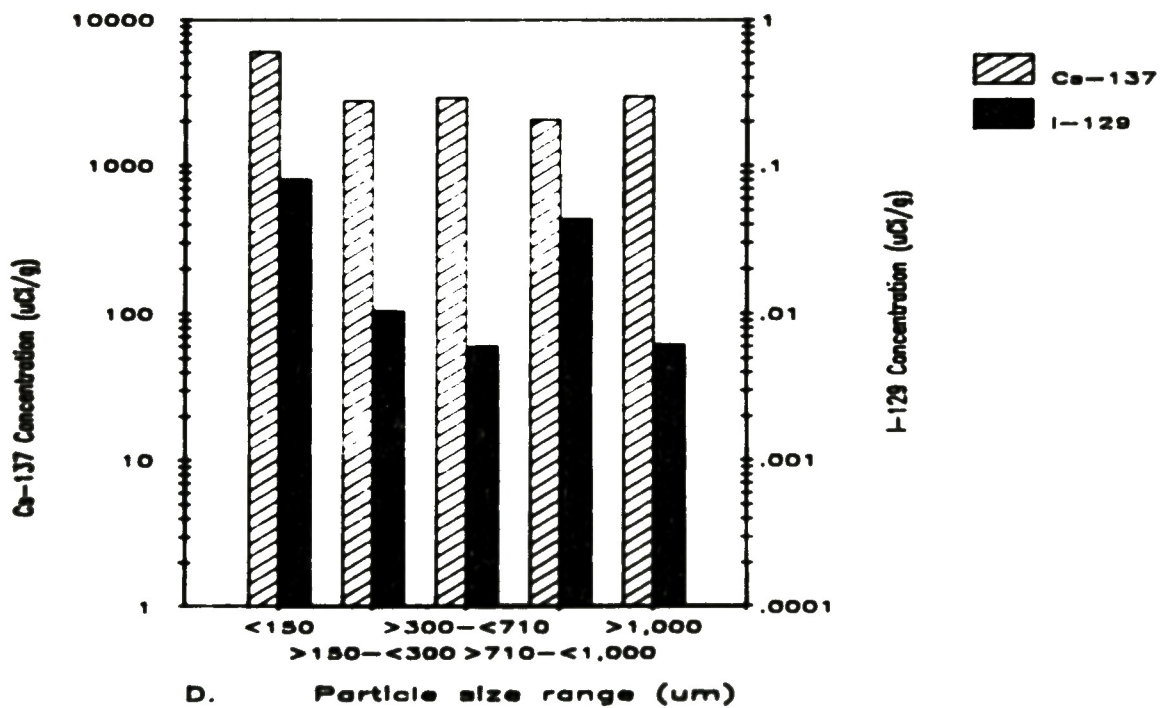
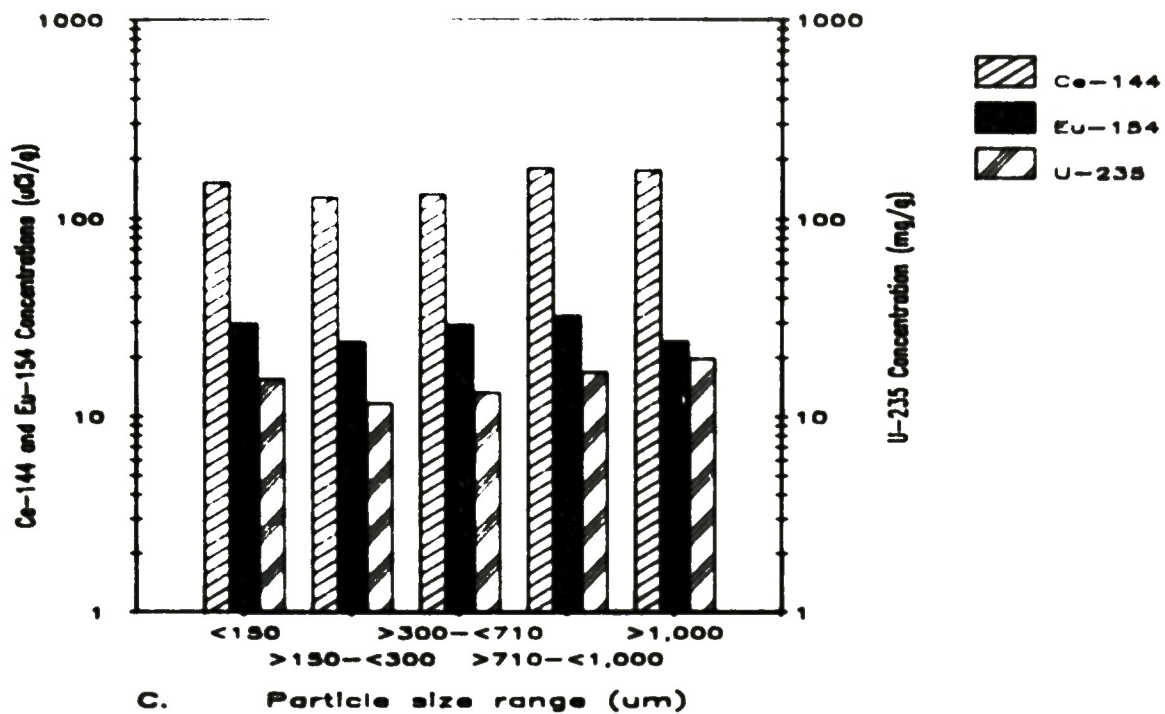


Figure 5. Radionuclide and U-235 concentrations as a function of particle size (Continued)

7 times the surface area of the same mass of 1000- $\mu\text{m}$  particles. The fact that the concentrations of several relatively volatile radionuclides are highest in particles smaller than 150  $\mu\text{m}$  might be explained by the higher surface-area-to-mass ratio of the 150- $\mu\text{m}$  particles. The data suggest that significant quantities of the Cs-137, I-129, Ru-106, and Sb-125 associated with the particles smaller than 150  $\mu\text{m}$  are deposited on the surfaces of the particles.

Some radionuclides indicate relatively consistent concentrations, whereas others are more variable. Plot A in Figure 5 shows that the concentrations of Cs-137 in particles larger than 150  $\mu\text{m}$  are comparable, and that the concentration of Ce-144 remains essentially constant over the entire range of particle sizes analyzed. The concentrations of Co-60, Sr-90, Ru-106, and Sb-125, on the other hand, exhibit more variation (see Plot B, Figure 5). The concentrations of Co-60 in particles smaller than 150  $\mu\text{m}$  and larger than 1000  $\mu\text{m}$  are between a factor of 5 and 10 lower than the Co-60 concentrations measured in the 3 intermediate particle-size ranges, which collectively have an average Co-60 concentration of 64.3  $\mu\text{Ci/g}$ . The concentrations of Sr-90 in the 710 to 1000 and >1000  $\mu\text{m}$  size ranges, which were measured to be 6.0 and 5.7 mCi/g, respectively, are about a factor of two higher than the corresponding concentrations measured in the three smaller particle-size ranges. Ruthenium-106 concentrations for the 5 particle-size groups range from a low of 49  $\mu\text{Ci/g}$  for the 150 to 300- $\mu\text{m}$  particle-size group to a high of 161  $\mu\text{Ci/g}$  for the <150- $\mu\text{m}$  size group. Antimony-125 is the only radionuclide whose concentrations appear to exhibit a trend. Plot B in Figure 5 shows that the concentration of Sb-125 decreases with increasing particle size. Its concentration is about 369  $\mu\text{Ci/g}$  in particles <150  $\mu\text{m}$ , whereas it is only about 45  $\mu\text{Ci/g}$  in particles >1000  $\mu\text{m}$ .

Table 4 presents steam-generator-debris radionuclide concentrations normalized to measured uranium concentrations, the results being expressed in units of  $\mu\text{Ci}$  per g of uranium. For each sample, the total uranium concentration was determined by dividing the U-235 concentration listed in Table 3 by an assumed U-235 enrichment. An enrichment of 0.0264 (i.e.,

TABLE 4. RADIONUCLIDE CONCENTRATIONS NORMALIZED TO URANIUM CONCENTRATIONS ( $\mu\text{Ci/g uranium}$ )<sup>a</sup>

Particle Size ( $\mu\text{m}$ )	Sample Mass (g)	( $\mu\text{Ci/g uranium}$ )									
		Co-60	Sr-90	Pu-106	Sr-125	U-129	Cs-134	Cs-137	Ce-144	Eu-154	Eu-155
<150	3 700 $\pm$ .02	2.08 $\pm$ .01	7.00 $\pm$ .03	2.74 $\pm$ .02	6.79 $\pm$ .02	1.38 $\pm$ .01	2.03 $\pm$ .02	1.03 $\pm$ .04	2.59 $\pm$ .02	5.04 $\pm$ .01	6.71 $\pm$ .01
>150 to <300	5 480 $\pm$ .02	1.55 $\pm$ .02	8.49 $\pm$ .03	1.11 $\pm$ .02	5.03 $\pm$ .02	2.37 $\pm$ .02	1.28 $\pm$ .02	6.25 $\pm$ .03	2.89 $\pm$ .02	5.40 $\pm$ .01	3.63 $\pm$ .01
>300 to <710	1 185 $\pm$ .01	1.02 $\pm$ .02	6.15 $\pm$ .03	1.15 $\pm$ .02	3.93 $\pm$ .02	1.20 $\pm$ .02	1.19 $\pm$ .02	5.77 $\pm$ .03	2.64 $\pm$ .02	5.03 $\pm$ .01	3.37 $\pm$ .01
>710 to <1,000	4 010 $\pm$ .02	1.14 $\pm$ .02	9.36 $\pm$ .03	9.97 $\pm$ .01	6.56 $\pm$ .01	6.80 $\pm$ .02	6.03 $\pm$ .01	3.22 $\pm$ .03	2.81 $\pm$ .02	5.88 $\pm$ .01	3.41 $\pm$ .01
>1,000	7 630 $\pm$ .02	4.11 $\pm$ .01	5.92 $\pm$ .03	7.79 $\pm$ .00	7.31 $\pm$ .01	7.03 $\pm$ .03	7.39 $\pm$ .01	4.28 $\pm$ .01	1.89 $\pm$ .02	2.45 $\pm$ .01	4.33 $\pm$ .01
>1,000	2 233 $\pm$ .01	3.44 $\pm$ .01	8.78 $\pm$ .03	1.39 $\pm$ .02	7.06 $\pm$ .01	2.83 $\pm$ .04	9.78 $\pm$ .01	6.41 $\pm$ .03	2.46 $\pm$ .02	3.09 $\pm$ .01	1.18 $\pm$ .01
>1,000	1 342 $\pm$ .01	3.55 $\pm$ .00	1.27 $\pm$ .04	1.77 $\pm$ .02	4.84 $\pm$ .01	4.47 $\pm$ .03	4.02 $\pm$ .01	1.93 $\pm$ .03	2.77 $\pm$ .02	5.44 $\pm$ .01	2.78 $\pm$ .01
>1,000	2 764 $\pm$ .01	7.72 $\pm$ .00	6.99 $\pm$ .03	1.28 $\pm$ .02	5.72 $\pm$ .01	5.42 $\pm$ .03	3.26 $\pm$ .01	1.98 $\pm$ .03	2.11 $\pm$ .02	3.00 $\pm$ .01	1.51 $\pm$ .01
>1,000	2 303 $\pm$ .01	2.87 $\pm$ .01	7.90 $\pm$ .03	9.10 $\pm$ .00	1.80 $\pm$ .01	1.32 $\pm$ .03	2.10 $\pm$ .01	1.13 $\pm$ .03	2.25 $\pm$ .02	8.57 $\pm$ .00	3.20 $\pm$ .01
>1,000	2 579 $\pm$ .01	6.19 $\pm$ .01	8.25 $\pm$ .03	1.55 $\pm$ .02	7.62 $\pm$ .01	1.84 $\pm$ .02	1.21 $\pm$ .02	6.85 $\pm$ .03	2.78 $\pm$ .02	3.79 $\pm$ .01	1.61 $\pm$ .01
>1,000	2 400 $\pm$ .01	9.90 $\pm$ .01	1.81 $\pm$ .03	1.21 $\pm$ .02	6.43 $\pm$ .01	1.73 $\pm$ .02	8.93 $\pm$ .01	5.94 $\pm$ .03	1.79 $\pm$ .02	2.66 $\pm$ .01	1.20 $\pm$ .01
Average <sup>b</sup>		1.19 $\pm$ .01	7.48 $\pm$ .03	1.05 $\pm$ .02	5.83 $\pm$ .01	7.74 $\pm$ .03	5.75 $\pm$ .01	3.47 $\pm$ .03	2.30 $\pm$ .02	3.04 $\pm$ .01	2.26 $\pm$ .01
Stand Dev		1.51 $\pm$ .01	3.03 $\pm$ .03	6.35 $\pm$ .01	1.87 $\pm$ .01	6.73 $\pm$ .03	4.16 $\pm$ .01	2.62 $\pm$ .03	3.66 $\pm$ .01	1.29 $\pm$ .01	1.12 $\pm$ .01

<sup>a</sup> Uranium concentration determined using NAA method.

<sup>b</sup> Average concentrations for >1,000 particles only.

2.64%) was assumed for the purpose of calculation; this enrichment has been shown to yield the most credible total uranium concentrations.<sup>7</sup> The data in Table 4 show that the more refractory radionuclides (i.e., Sr-90, Ce-144, Eu-154, and Eu-155) exhibit normalized concentrations still essentially independent of particle size. This indicates that the relative quantities of these radionuclides deposited on the surfaces of the particles are small. It also indicates that particle size did not significantly influence the leachability of these refractory radionuclides. In contrast, the normalized concentrations of Cs-134, Cs-137, and Ru-106 for the <150- $\mu\text{m}$  particle-size group are between a factor of 2 and 10 higher than their corresponding concentrations in the larger particle-size groups. As previously mentioned, particles 150  $\mu\text{m}$  in size have a surface-area-to-mass ratio about a factor of 7 greater than that for 1000  $\mu\text{m}$  particles. The elevated concentrations of Cs-134, Cs-137, and Ru-106 in particles <150  $\mu\text{m}$  might result from the fact that relatively large fractions of the activities of these radionuclides are plated out on the surfaces of the particles.

In order to estimate what fraction of the activity in the steam-generator sample can be accounted for by the activity retained by the fuel in the sample, the normalized data presented in Table 4 were divided by the corresponding concentrations calculated, using ORIGEN2 results. For each fission product, the activity calculated using ORIGEN2 was decay-corrected to April 1, 1987, and then divided by the preaccident mass of uranium in the core, which is estimated to be  $8.375 \text{ E}+07 \text{ g}$ .<sup>2</sup> Because both the measured and theoretical fission product concentrations are expressed as  $\mu\text{Ci}$  per g uranium, their ratio is dimensionless. If all of the activity of a particular radionuclide is considered to be associated with fuel, then the ratio can be interpreted as the maximum fraction of the activity of the radionuclide considered to have been retained by the fuel.

The calculated maximum radionuclide retentions are presented in Table 5. The data in Table 5 show that the measured concentrations of the majority of the radionuclides, expressed as  $\mu\text{Ci}$  per g uranium, are higher in particles smaller than 150  $\mu\text{m}$  than can be accounted for by the



TABLE 5. RETENTIONS OF FISSION PRODUCTS BASED ON THEIR THEORETICAL CORE AVERAGE CONCENTRATIONS IN THE FUEL<sup>a</sup>

Particle Size (µm)	Sample Mass (g)	Sr-90	Ru-106	Sb-125	I-129	Cs-134	Cs-137	Eu-154	U-155
<150	3.700 ± 0.2	9.51 ± 0.1	1.67 ± 0.0	3.13 ± 0.0	5.04 ± 0.1	1.30 ± 0.0	1.22 ± 0.0	1.23 ± 0.0	8.50 ± 0.1
>150 to <300	5.400 ± 0.2	1.15 ± 0.0	6.76 ± 0.1	2.50 ± 0.0	8.86 ± 0.0	8.19 ± 0.1	7.40 ± 0.1	1.37 ± 0.0	9.10 ± 0.1
>300 to <710	1.185 ± 0.1	8.36 ± 0.1	6.99 ± 0.1	1.95 ± 0.0	4.39 ± 0.0	7.61 ± 0.1	6.83 ± 0.1	1.25 ± 0.0	9.84 ± 0.1
>710 to <1,000	4.010 ± 0.2	1.27 ± 0.0	6.08 ± 0.1	3.76 ± 0.1	2.49 ± 0.1	3.87 ± 0.1	3.81 ± 0.1	1.33 ± 0.0	8.56 ± 0.1
>1,000	7.630 ± 0.2	8.04 ± 0.1	4.75 ± 0.2	3.64 ± 0.1	2.57 ± 0.0	4.74 ± 0.3	5.06 ± 0.3	8.96 ± 0.1	4.13 ± 0.1
>1,000	2.233 ± 0.1	1.19 ± 0.0	8.49 ± 0.1	3.51 ± 0.1	1.04 ± 0.1	6.27 ± 0.1	7.59 ± 0.1	1.18 ± 0.0	5.21 ± 0.1
>1,000	1.342 ± 0.1	1.72 ± 0.0	1.08 ± 0.0	2.41 ± 0.1	1.64 ± 0.0	2.58 ± 0.1	2.28 ± 0.1	1.31 ± 0.0	9.18 ± 0.1
>1,000	2.764 ± 0.1	9.50 ± 0.1	7.79 ± 0.1	2.85 ± 0.1	1.99 ± 0.0	2.09 ± 0.1	2.35 ± 0.1	1.00 ± 0.0	5.06 ± 0.1
>1,000	2.303 ± 0.1	1.07 ± 0.0	5.55 ± 0.2	8.93 ± 0.2	4.84 ± 0.1	1.34 ± 0.1	1.33 ± 0.1	1.07 ± 0.0	1.45 ± 0.1
>1,000	2.579 ± 0.1	1.12 ± 0.0	9.45 ± 0.1	3.79 ± 0.1	6.73 ± 0.0	7.73 ± 0.1	8.11 ± 0.1	1.32 ± 0.0	6.39 ± 0.1
>1,000	2.400 ± 0.1	2.45 ± 0.1	7.36 ± 0.1	3.20 ± 0.1	6.33 ± 0.0	5.72 ± 0.1	7.03 ± 0.1	8.51 ± 0.1	4.49 ± 0.1
Average <sup>b</sup> :		1.02 ± 0.0	6.42 ± 0.1	2.90 ± 0.1	2.83 ± 0.0	3.68 ± 0.1	4.11 ± 0.1	1.09 ± 0.0	5.13 ± 0.1
Stand Dev.:		4.12 ± 0.1	3.87 ± 0.1	9.32 ± 0.2	2.47 ± 0.0	2.66 ± 0.1	3.10 ± 0.1	1.74 ± 0.1	2.17 ± 0.1

a. Core inventory was calculated using the ORIGEN-2 Code. Data was taken from Table B 1 of GMD-057, November 1986. The mass of uranium in the core prior to the accident that was used in the normalization calculations is 8.375 ± 0.7 g.

b. Average retentions for >1,000 µm particles only.

activities retained by the fuel. For example, the results for I-129 indicate that the normalized concentration of I-129 in particles smaller than 150  $\mu\text{m}$  is about 50 times higher than the average concentration of I-129 in the fuel at the time of the accident. Similar results for other radionuclides for the same particle-size fraction are Ru-106, 1.67; Sb-125, 3.13; Cs-134, 1.30; Cs-137, 1.22; and Ce-144, 1.23. As previously mentioned, these results might be explained by activities deposited on the surfaces of the particles, given the fact that the surface-area-to-mass ratio increases with diminishing particle size. The data presented in Table 5 indicate that the concentrations of Sr-90 and Eu-154 in the fuel in particles smaller than 150  $\mu\text{m}$  are about equal to their average concentrations in the fuel at the time of the accident.

### 3.3 Elemental Analyses

The results of the ICP elemental analyses of the sieved fractions are presented in Table 6. Concentrations are expressed as Wt%. The sum of the concentrations of the elements detected in a given sample do not normally add up to 100%. Based on the results presented in Table 6, the cumulative weight percents of the elements quantified in each sample are <150  $\mu\text{m}$ , 82.6 Wt%; >150 to <300  $\mu\text{m}$ , 61.9 Wt%; >300 to <710  $\mu\text{m}$ , 64.6 Wt%; >710 to <1000  $\mu\text{m}$ , 100.1 Wt%, and >1000  $\mu\text{m}$ , 82.2 Wt%. The cumulative concentrations for a given sample are expected to be less than 100% because major elements such as oxygen could not be measured using the ICP technique. The total uncertainty associated with the element concentrations reported in Table 6 is 10 to 15%.<sup>2</sup>

The concentrations of U, Zr, and Sn in the steam generator debris sample are plotted as a function of particle size in Figure 6, Plot A. Although the data exhibit anomalies (e.g., the concentrations of Zr and Sn for the >710 to <1000  $\mu\text{m}$  group appear to be too high), two trends are apparent: (1) the concentration of U increases with increasing particle size, and (2) the concentrations of Zr and Sn decrease with increasing particle size. The value of the Zr/U ratio for the 7 individual particles larger than 1000  $\mu\text{m}$  ranges from 0.003 to 0.50. Five of the 7 particles

TABLE 6. CONCENTRATIONS OF ELEMENTS IN DEBRIS COLLECTED FROM THE "B" STEAM GENERATOR UPPER TUBE SHEET (wt%)

Particle Size ( $\mu$ m)	Sample Mass (g)	Ag	Al	B	Cd	Cr	Cu	Fe	Gd	In
<150	3.700 E-02	2.03 E+00	<1.4 E+00	<1.4 E+00	6.09 E-01	<2.0 E+00	6.09 E-01	2.23 E-01	<1.8 E+00	<4.9 E+00
>150 to <300	5.480 E-02	1.64 E+00	<9.6 E-01	<9.6 E-01	4.10 E-01	<1.4 E+00	2.74 E-01	1.23 E+00	<1.2 E+00	<3.3 E+00
>300 to <710	1.185 E-01	7.60 E-01	8.23 E-01	<4.4 E-01	3.16 E-01	<6.3 E-01	1.90 E-01	1.52 E+00	<5.7 E-01	<1.5 E+00
>710 to <1,000	4.010 E-02	<4.0 E-01	1.50 E+00	<1.3 E+00	1.87 E-01	<1.9 E+00	3.74 E-01	7.48 E-01	<1.7 E+00	<4.5 E+00
>1,000	7.630 E-02	<2.0 E-01	<6.9 E-01	<6.9 E-01	9.83 E-02	<9.8 E-01	1.97 E-01	2.95 E-01	<8.8 E-01	<2.4 E+00
>1,000	2.233 E-01	<6.7 E-02	<2.4 E-01	<2.4 E-01	3.36 E-02	<3.3 E-01	6.72 E-02	<6.7 E-02	<3.0 E-01	<8.1 E-01
>1,000	1.342 E-01	<1.1 E-01	<3.9 E-01	<3.9 E-01	1.12 E-01	<5.6 E-01	5.59 E-02	<1.1 E-01	<5.0 E-01	<1.3 E-01
>1,000	2.264 E-01	<6.6 E-02	<2.3 E-01	<2.3 E-01	3.31 E-02	<3.3 E-01	3.31 E-02	<6.6 E-02	<3.0 E-01	<7.9 E-01
>1,000	2.303 E-01	<6.5 E-02	4.20 E-01	<2.3 E-01	9.73 E-02	<3.2 E-01	6.49 E-02	2.27 E-01	<2.9 E-01	<7.8 E-01
>1,000	2.579 E-01	<5.8 E-02	<2.0 E-01	<2.0 E-01	2.91 E-02	<2.9 E-01	8.72 E-02	<5.8 E-02	<2.6 E-01	<7.0 E-01
>1,000	2.400 E-01	<6.3 E-02	<2.2 E-01	<2.2 E-01	<3.1 E-02	<3.1 E-01	9.38 E-02	<6.3 E-02	<2.8 E-01	<7.5 E-01
Average <sup>a</sup> :	-	-	4.20 E-01	--	6.72 E-02	--	8.56 E-02	2.61 E-01	--	--
Std. Dev.:	-	--	--	--	3.56 E-02	--	4.91 E-02	1.40 E-02	--	--

TABLE 6. (Continued)

Particle Size ( $\mu\text{m}$ )	Sample Mass (g)	Mn	Mo	Ni	Nb	Si	Sn	Te	U	Zr
<150	3.700 E-02	4.10 E-01	<4.9 E+00	<1.2 E+00	<8.1 E-01	<1.2 E+00	9.13 E+00	<5.5 E+00	5.87 E+01	8.92 E+00
>150 to <300	5.480 E-02	2.70 E-01	<3.3 E+00	<8.2 E-01	<5.5 E-01	<8.2 E-01	5.34 E+00	<3.7 E+00	4.43 E+01	8.48 E+00
>300 to <710	1.185 E-01	1.30 E-01	<1.5 E+00	<3.8 E-01	<2.5 E-01	<3.8 E-01	2.91 E+00	<1.7 E+00	5.04 E+01	7.59 E+00
>710 to <1,000	4.010 E-02	3.70 E-01	<4.5 E+00	<1.1 E+00	<7.5 E-01	<1.1 E+00	6.54 E+00	<5.0 E+00	6.40 E+01	2.64 E+01
>1,000	7.630 E-02	2.00 E-01	<2.4 E+00	<5.9 E-01	<3.9 E-01	<5.9 E-01	4.03 E+00	<2.5 E+00	3.53 E+01	1.76 E+01
>1,000	2.233 E-01	6.70 E-02	<8.1 E-01	<2.0 E-01	<1.3 E-01	<2.0 E-01	1.24 E+00	<9.1 E-01	8.83 E+01	4.03 E-01
>1,000	1.342 E-01	1.10 E-01	<1.3 E+00	<3.4 E-01	<2.2 E-01	<3.4 E-01	2.40 E+00	<1.5 E+00	8.60 E+01	7.83 E-01
>1,000	2.264 E-01	6.60 E-02	<7.9 E-01	<2.0 E-01	<1.3 E-01	<2.0 E-01	1.46 E+00	<8.9 E-01	8.37 E+01	1.89 E+00
>1,000	2.303 E-01	6.50 E-02	<7.8 E-01	<1.9 E-01	<1.3 E-01	<1.9 E-01	7.13 E-01	<8.8 E-01	5.68 E+01	9.37 E+00
>1,000	2.579 E-01	5.80 E-02	<7.0 E-01	<1.7 E-01	<1.2 E-01	<1.7 E-01	1.22 E+00	<7.9 E-01	8.7 E+01	2.91 E-01
>1,000	<u>2.400 E-01</u>	<u>6.30 E-02</u>	<u>&lt;7.5 E-01</u>	<u>&lt;1.9 E-01</u>	<u>&lt;1.3 E-01</u>	<u>&lt;1.9 E-01</u>	<u>1.56 E+00</u>	<u>&lt;8.4 E-01</u>	<u>8.86 E+01</u>	<u>2.50 E-01</u>
	Average <sup>a</sup> :	8.99 E-02	--	--	--	--	1.80 E+00	--	7.51 E+01	4.37 E+00
	Std. Dev.:	4.78 E-02	--	--	--	--	1.02 E+00	--	1.93 E+01	6.19 E+00
Recombined	4.032 E+01	5.90 E-02	<7.1 E-01	6.76 E-01	1.18 E-01	4.40 E-01	<5.9 E-01	<7.9 E-01	6.52 E+01	3.28 E+00

a. Average concentrations of >1,000  $\mu\text{m}$  particles only. Less than values were ignored when computing average values.



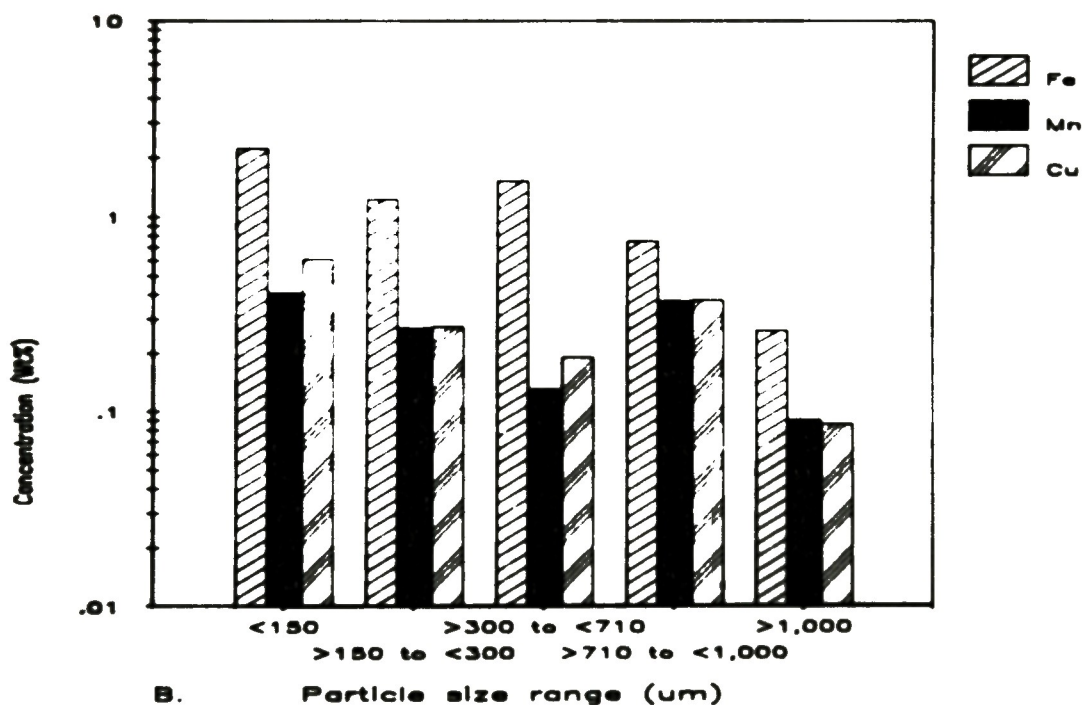
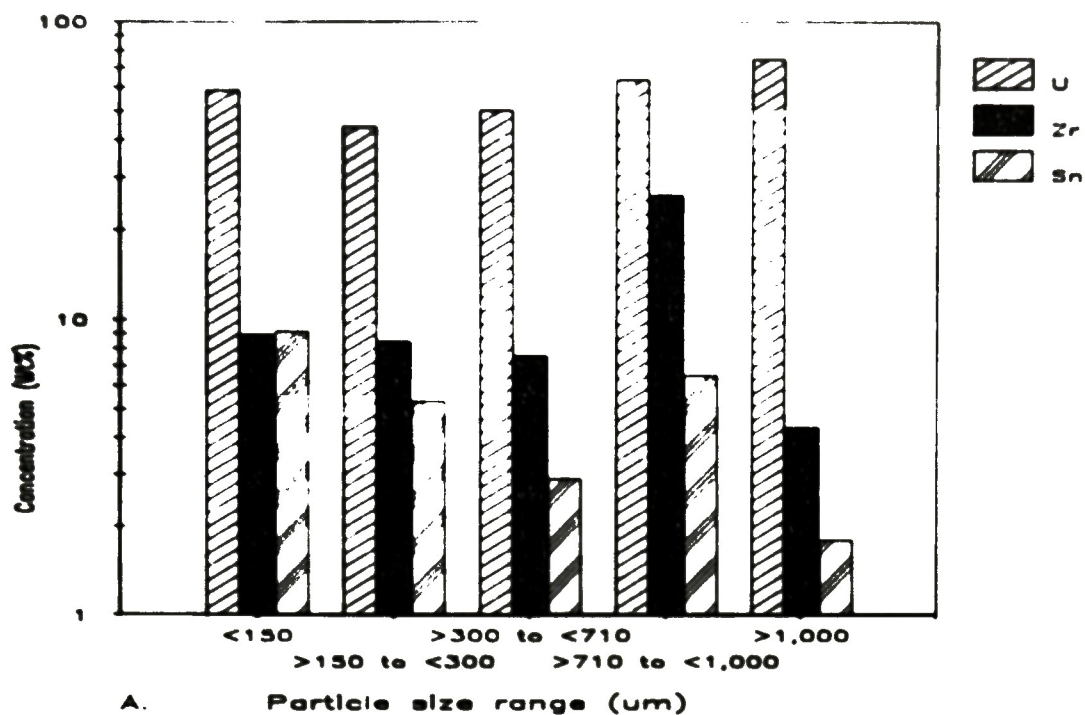


Figure 6. Element concentrations as a function of particle size.

larger than 1000  $\mu\text{m}$  are particles of fuel that have masses ranging from about 0.13 to 0.26 g. The Zr/U ratio has a maximum value of 0.02 for these 5 particles. Two samples exhibit relatively high Zr concentrations. The sieve fraction >710 to <1000  $\mu\text{m}$  has a Zr concentration of 26.4 Wt%, and one of the particles larger than 1000  $\mu\text{m}$  has a Zr concentration of 17.6 Wt%.

The Ag-In-Cd control rod materials collectively account for approximately 2.1 Wt% of the core mass. Because they are relatively volatile, it is likely they were transported from the reactor core to the steam generator as aerosols. The alloy melts at the relatively low temperature of 799° C, and the control rod cladding, which is 304 stainless steel, melts at a temperature between 1399 and 1454° C. The boiling temperatures of elemental Ag, In, and Cd at atmospheric pressure are 2212, 2000, and 765° C.

The data presented in Table 6 show that the concentrations of Ag and Cd in the steam generator debris sample are highest for particles smaller than 150  $\mu\text{m}$ . Silver was not detected in particles larger than 710  $\mu\text{m}$ , but for the three particle size groups that contained detectable quantities of Ag, the concentration of Ag decreases with increasing particle size. For the particle size groups below 710  $\mu\text{m}$ , the concentration of Ag is a factor of 2 or more greater than the concentration of Cd. The concentration of Cd decreases nearly linearly with increasing particle size. For particles smaller than 150  $\mu\text{m}$ , it has a concentration of 0.61 Wt%, which is almost 6 times its core average concentration, whereas its average concentration in the 7 particles larger than 1000  $\mu\text{m}$  is about a factor of ten less, being only 0.07 Wt%.

As previously mentioned, Al is present in the core as the burnable poison  $\text{Al}_2\text{O}_3\text{-B}_4\text{C}$  burnable poison material. A second burnable poison also present in the  $\text{UO}_2$  in four experimental fuel assemblies is  $\text{Gd}_2\text{O}_3\text{-UO}_2$ . Aluminum was detected in only one of the steam-generator debris particles larger than 1000  $\mu\text{m}$  and in only two of the sieve

fractions containing particles smaller than 1000  $\mu\text{m}$ . The Al concentrations for these samples range from 0.42 Wt% (1000- $\mu\text{m}$  particle) to 1.50 Wt% (>710 to <1000- $\mu\text{m}$  sieve fraction). Given the fact that the vacuum apparatus used to collect the debris sample was equipped with an Al nozzle, the data for Al must be used with caution.

The principal structural material elements detected in the steam-generator debris samples are Ni, Si, Fe, Nb, and Mn. Chromium, which is a major constituent of stainless steel and Inconel structures, was not detected, probably owing to the high detection limit for Cr in ICP analysis, which results from the location of the emission line measured in the spectrum.

#### 4. OBSERVATIONS AND CONCLUSIONS

The physical, chemical, and radiochemical analyses performed on the samples of loose particulate debris collected from the upper tube sheet of the B-loop steam generator during March 1987 provide significant information on the physical characteristics and chemical composition of the debris. Because many of the analyses performed on the steam-generator debris sample were also performed on the samples of debris collected from the core upper debris bed, it is possible to compare the compositions of the two types of debris samples. Since it is likely that the loose particulate matter recovered from the steam-generator upper tube sheet was transported to the steam generator shortly after the 2-B reactor coolant pump was turned on 174 min into the accident, the analysis results for the sample provide a basis for updating our knowledge of the condition of the core at about 174 min into the accident. The principal observations and conclusions include the following:

Approximately 93 Wt% of the debris material is larger than 1000  $\mu\text{m}$ . The largest particles are particles of fuel that range in mass from 0.13 to 0.26 g.

The dominant activities in the samples are Cs-137 and Sr-90; their concentrations are about 3.5 and 2.0 mCi/g, respectively.

Concentrations of the relatively volatile radionuclides I-129, Cs-134, Cs-137, and Sb-125 are considerably higher in the steam generator debris samples than in the samples of debris collected from the core upper debris bed. Their concentrations are highest in the particles smaller than 150  $\mu\text{m}$ .

The average concentration of I-129 in the steam generator debris samples is about a factor of 17 higher than its average concentration in the samples from the core upper debris bed. The concentration of I-129 in the steam generator debris sample is about a factor of 4 higher than its predicted core average concentration.



Antimony-125 concentration decreases with increasing particle size and is highest in particles smaller than 150  $\mu\text{m}$ .

Significant fractions of the activities of the relatively more volatile radionuclides, such as I-129, Cs-134, Cs-137, and Sb-125, are probably plated out on the surfaces of the particles in the steam generator debris sample.

The concentrations of Sr-90, Ce-144, Eu-154, and Eu-155, when normalized to uranium concentrations, are essentially independent of particle size. This indicates that the relative quantities of these radionuclides deposited on the surfaces of the particles are small and that particle size did not influence the leachability of the refractory radionuclides.

The U concentration in the debris from the steam generator is approximately equal to its core average value, which is about 65 Wt%.

The concentration of Zr in the steam generator-debris sample is about a factor of 5 lower than its core average concentration.

The concentrations of Ag and Cd in the steam-generator debris sample are significantly higher than their corresponding concentrations in the samples of debris collected from the core upper debris bed. The concentrations of these two relatively volatile elements are highest in particles smaller than 150  $\mu\text{m}$ , indicating that they were likely transported to the steam generator as aerosols.

## REFERENCES

1. D. W. Akers, et al., TMI-2 Core Debris Grab Samples--Examination and Analysis (Part 1), GEND-INF-075, September 1986.
2. E. L. Tolman, et al., TMI-2 Core Bore Acquisition Summary Report, EGG-TMI-7385, Rev. 1, February 1987.
3. E. L. Tolman, et al., TMI-2 Accident Scenario Update, EGG-TMI-7489, December 1986.
4. M. L. Russell, private communication, EG&G Idaho, Inc., November 24, 1987.
5. E. W. Killian and J. K. Hartwell, VASGAP, A Pulse-Height Gamma Ray Analysis Package for a VAX Computer, EG&G Idaho Report (to be published).
6. A. E. Proctor, Y. D. Harker, D. W. Akers, and J. W. Mandler, "Delayed Neutron Method for Measurement of Fissile/Fertile Content of Samples Ranging from Environmental to Irradiated Fuel," Proceedings of the Institute of Nuclear Materials Management, 1984 Annual Meeting, June 1, 1984.
7. R. J. Gehrke, private communication, EG&G Idaho, Inc., February 24, 1987.
8. D. W. Akers, et al., TMI-2 Core Debris Grab Samples--Examination and Analysis (Part 2), GEND-INF-075, September 1986.
9. D. H. Meikrantz, private communication, EG&G Idaho, Inc., May 5, 1987.
10. S. Langer, et al., TMI-2 Fission Product Inventory Program FY-85 Status Report, GEND-057, November 1986.

